Some properties of the global behaviour of conservative low dimensional systems

Carles Simó

Dept. Matemàtica Aplicada i Anàlisi, UB

carles@maia.ub.es

FoCM08

City University of Hong Kong

Hong Kong 080618

Contents

- **A sample of problems**
  - The Restricted Three-Body Problem: Trojans and Greeks, outer comets, asteroids, satellites
  - The Sitnikov problem
  - Bifurcations: the Hopf-saddle-node conservative unfolding and Michelson system
  - Fluid mechanics: the Rayleigh-Bénard problem
  - A paradigmatic example: the Hénon map
- **Analytic tools**
  - KAM theory: conditions for applicability
  - The splitting of separatrices
  - Key models and return maps

- **Computational tools**
  - Long time integrations: Taylor methods
  - Dynamics indicators: Lyapunov exponents, frequency analysis
  - Computing qp invariant curves
  - Curve fitting
- **Some details on the Hénon map**
  - A general overview
  - Near-integrable case
  - A low-order resonance
- **Open problems and conclusions**

A sample of problems

The Restricted Three-Body Problem: Trojans and Greeks, outer comets, asteroids, satellites

Hamiltonian in synodic coordinates (rotating coordinates)

$$H = \frac{1}{2}(p_x^2 + p_y^2) + y p_x - x p_y - \frac{1-\mu}{r_1} - \frac{\mu}{r_2}, \quad \text{on level} \quad H = -0.5(C - \mu(1-\mu)),$$

$$r_1 = ((x-\mu)^2 + y^2)^{1/2}, \quad r_2 = ((x-\mu+1)^2 + y^2)^{1/2}, \quad \mu = m_J/(m_S + m_J).$$

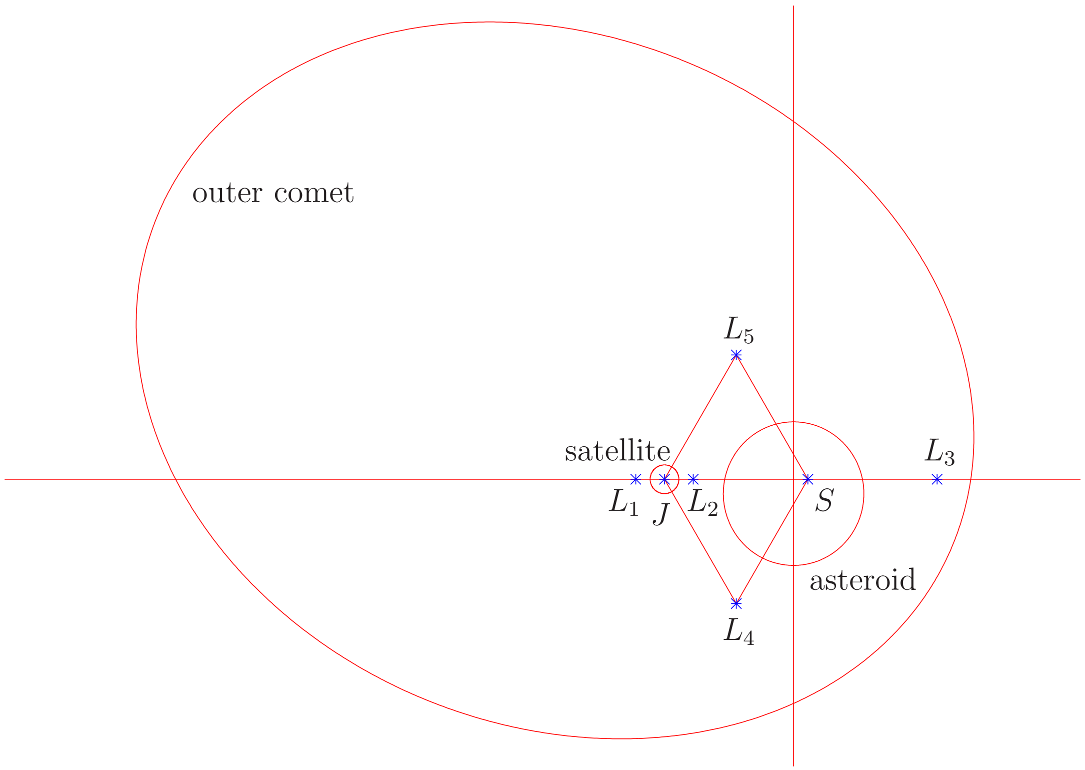

Questions

1) On a given level of energy: when the orbit of an asteroid, an outer comet, a satellite, is bounded? (no escape, no collision). Up to which e?

2) Triangular points L_4, L_5, close to Trojan and Greek asteroids. Linearly stable for $\mu \in [0, \mu_1]$, where

$$\mu_s = \omega_{\text{short}}/\omega_{\text{long}} = s, \qquad s \in \mathbb{N}.$$

$\omega_{\text{short}}, \omega_{\text{long}}$ = frequencies at $L_{4,5}$: $\left[(1 \pm (1 - 27\mu(1-\mu))^{1/2})/2\right]^{1/2}$.
Nonlinear stability for $\mu \in [0, \mu_1] \setminus \{\mu_2, \mu_3\}$. **Practical** stability in 3D.
Up to which distance do we have some kind of stability?

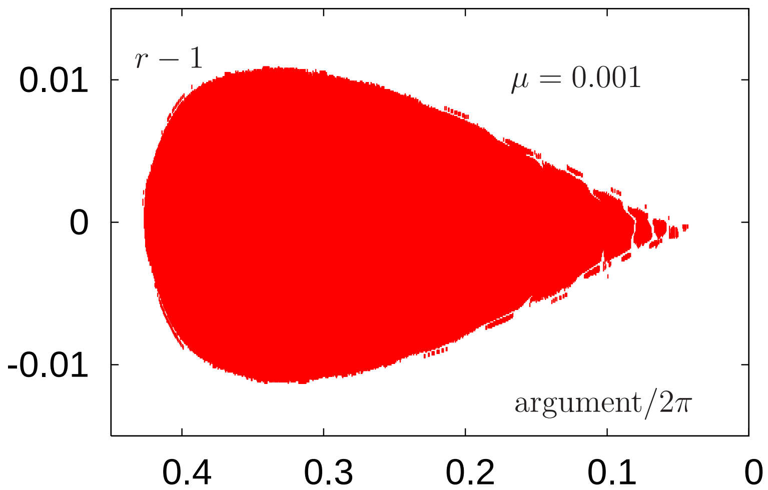

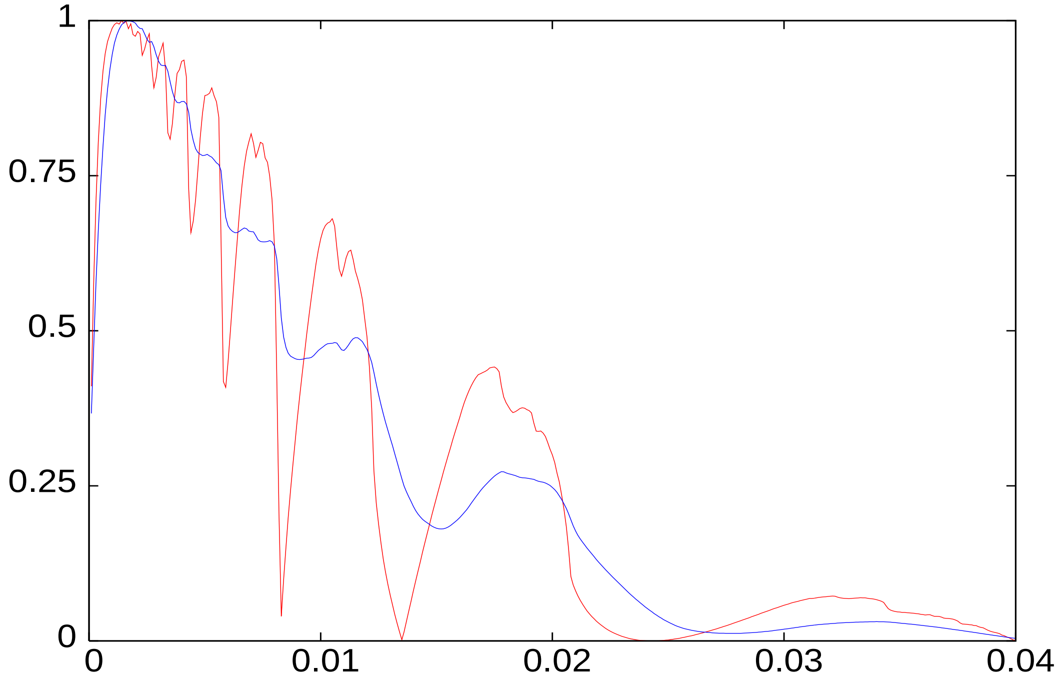

Normalised subsisting points. Planar case (in red): Maximal value, for $\mu = 0.0014$. Spatial case (in blue): Maximal value, for $\mu = 0.0017$. The role of resonances is clearly seen (2D, 3D differ)

Initial conditions: (r, α) polar coordinates w.r.t. centre of mass. Zero synodical velocity

The Sitnikov problem

Classical and popular problem. Relevant as first example of **oscillatory motion** (Chazy, Sitnikov, Alekseev, McGehee, Moser)

$$\ddot{z} = -\frac{z}{(z^2 + r(t)^2/4)^{3/2}}, \quad r(t) = 1 - e\cos(E), \quad t = E - e\sin(E).$$

Suitable Poincaré map: passages through $z = 0$: $(|v|_k, t_k) \longrightarrow (|v|_{k+1}, t_{k+1})$ (in polar coordinates), where $v = dz/dt$.

For $e = 0$, integrable, bounded motion iff $|v| < 2$.

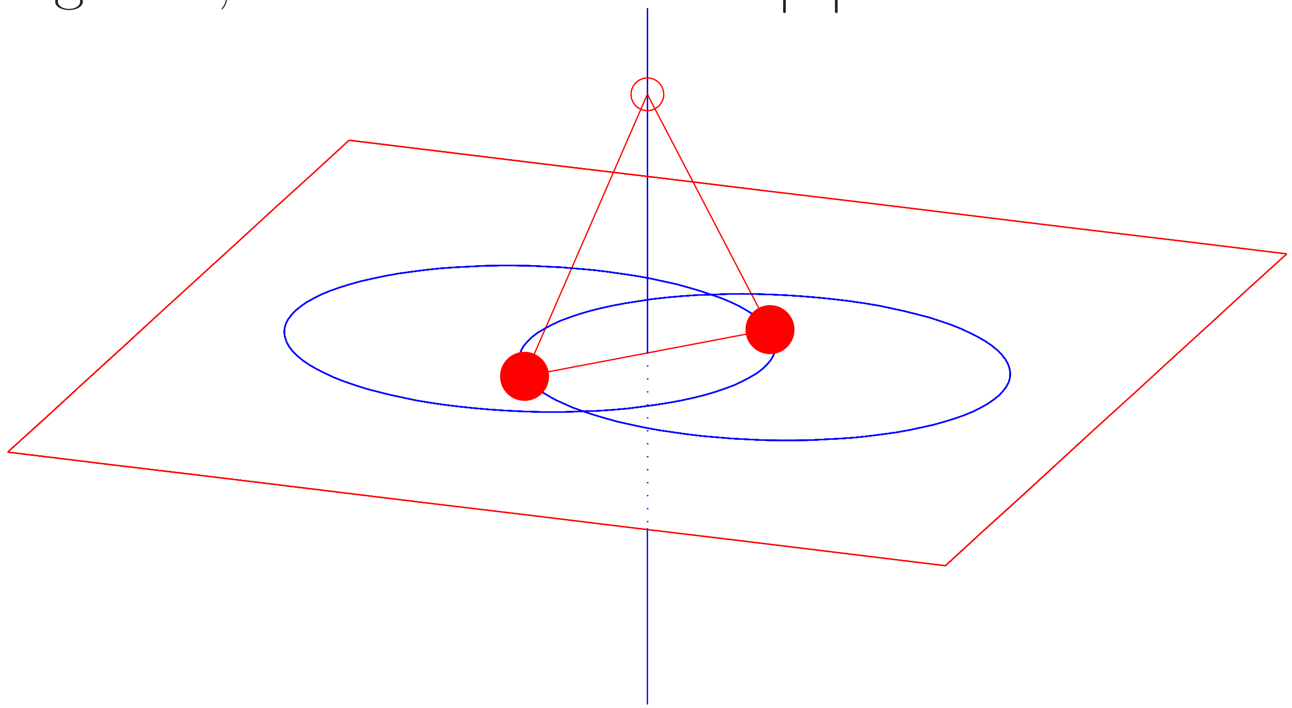

Global aspects

Up to which distance it is possible to find **rotational invariant curves (i.c.)**?

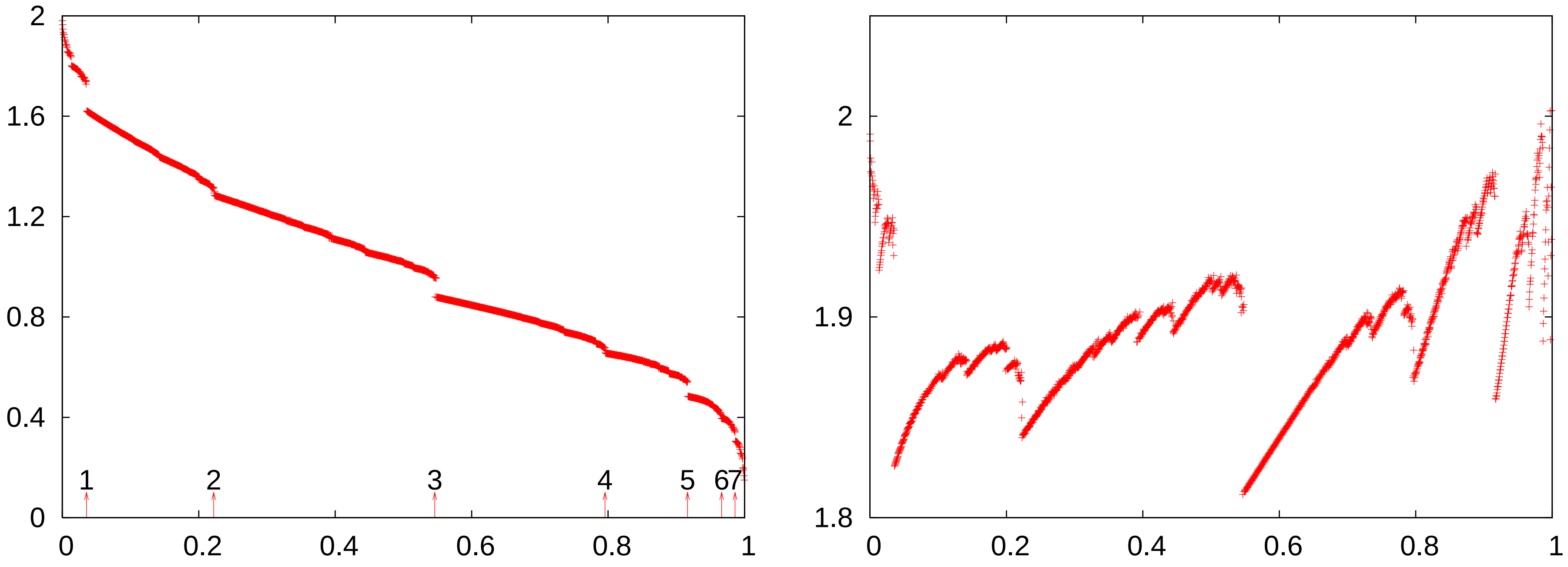

Left: $\approx$ maximal $|\dot{z}|$ on $E = \pi$ as a function of e.
Right: Idem but plotting $|\dot{z}|/(1-e)^{1/4} + \sqrt{e}$ vs e.

Infinitely many jumps. In left plot we mark places where i.c. confining islands of period $1, 2, \ldots, 7$ breakdown. Next plots show illustrations for some periods.

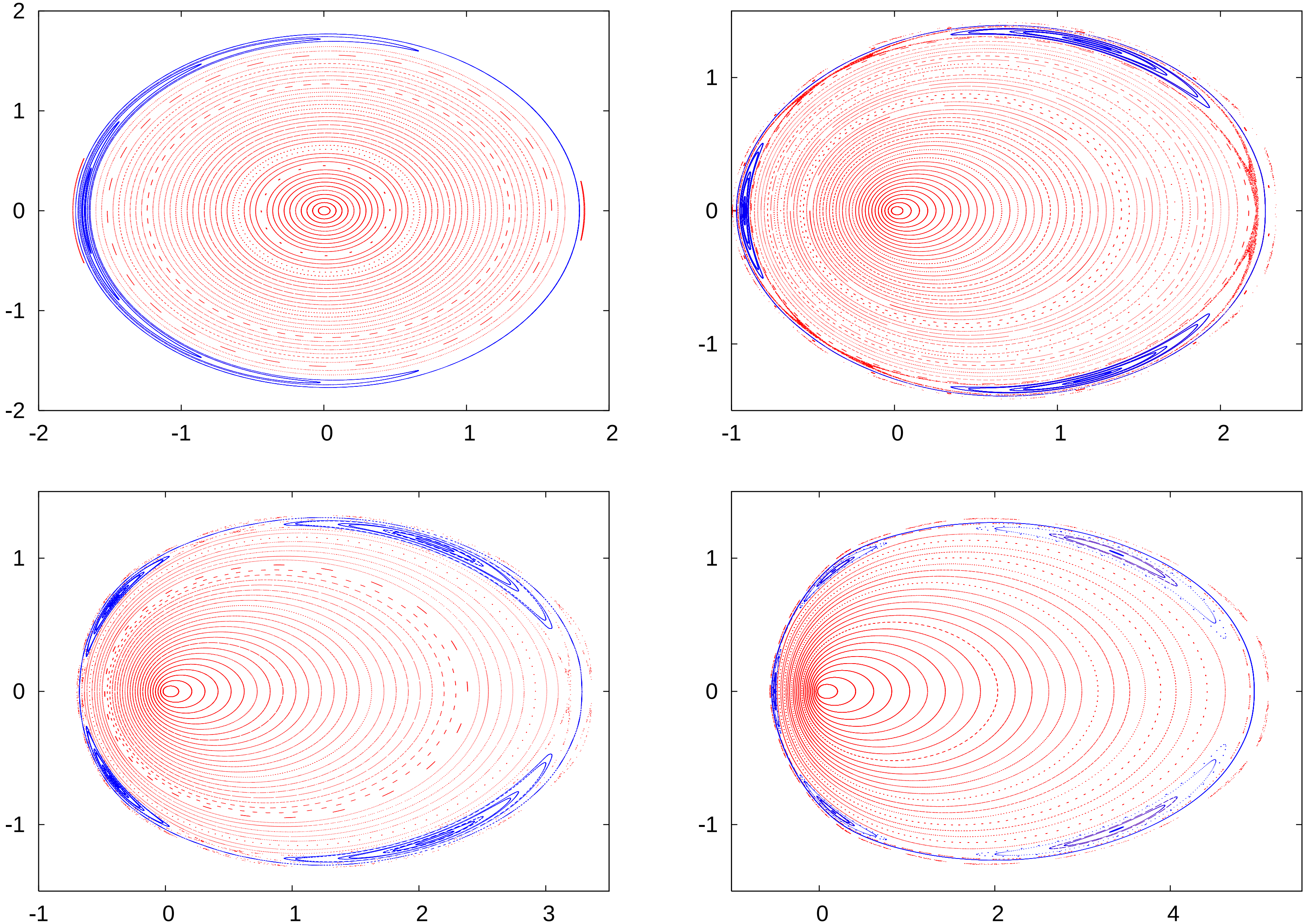

Poincaré maps for $e = 0.032, 0.540, 0.790, 0.910$, close to breakdown of i.c. outside islands of periods $1, 3, 4, 5$, respectively.

Bifurcations: the Hopf-saddle-node conservative unfolding

At a **HSN bifurcation** eigenvalues are $0, \pm i$. **Normal Forms**, formally rotationally invariant can be computed, and unfolded generically.
The **volume preserving** case helps to understand other cases.

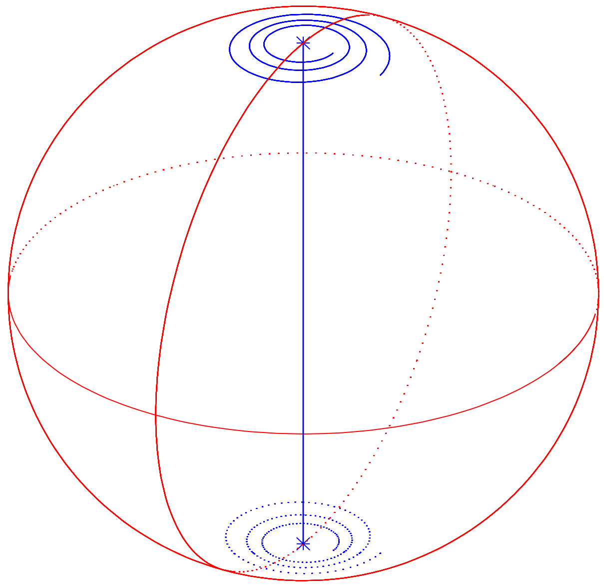

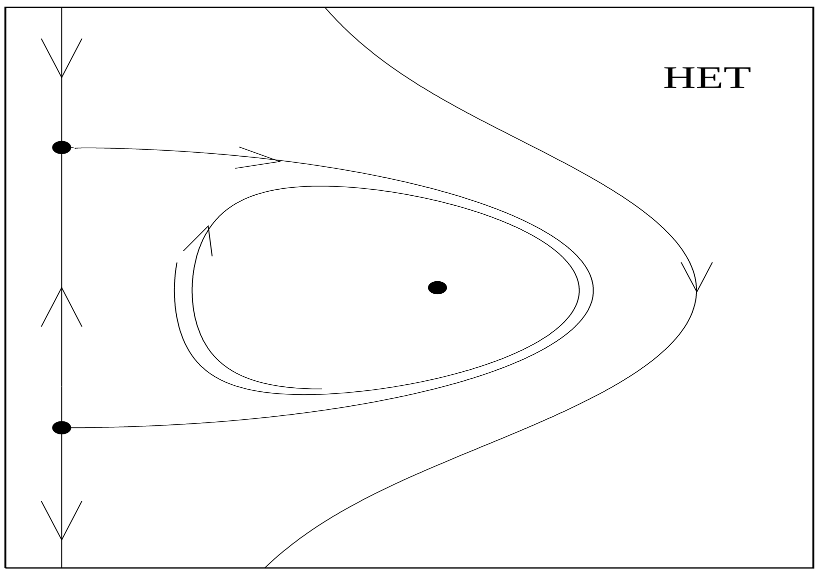

Left: **behaviour of the NF** to any order, conservative case. The 1D and 2D $W^{u,s}$ of south and north poles **do not split**. The system is integrable. Right: A meridian section for parameter values giving rise to **heteroclinic connections** in the general case. In the conservative one the domain between separatrices is foliated by i.c.

Michelson system

A simple model, representative enough, is **Michelson system**, appearing also as travelling waves in the **Kuramoto-Shivasinski** PDE.

$$x''' = -1 + ax' + x^2,\ a > 0.$$

It is convenient to use as parameter $\varepsilon = (-a)^{-3}$. The NF to any order has **connecting 2D and 1D** invariant manifolds of $(\pm 1, 0, 0)$. Real system has **splittings exponentially small in** ε (see Dumortier-Ibañez-Kokubu-S, in preparation). Plot: measure of confined domain vs ε.

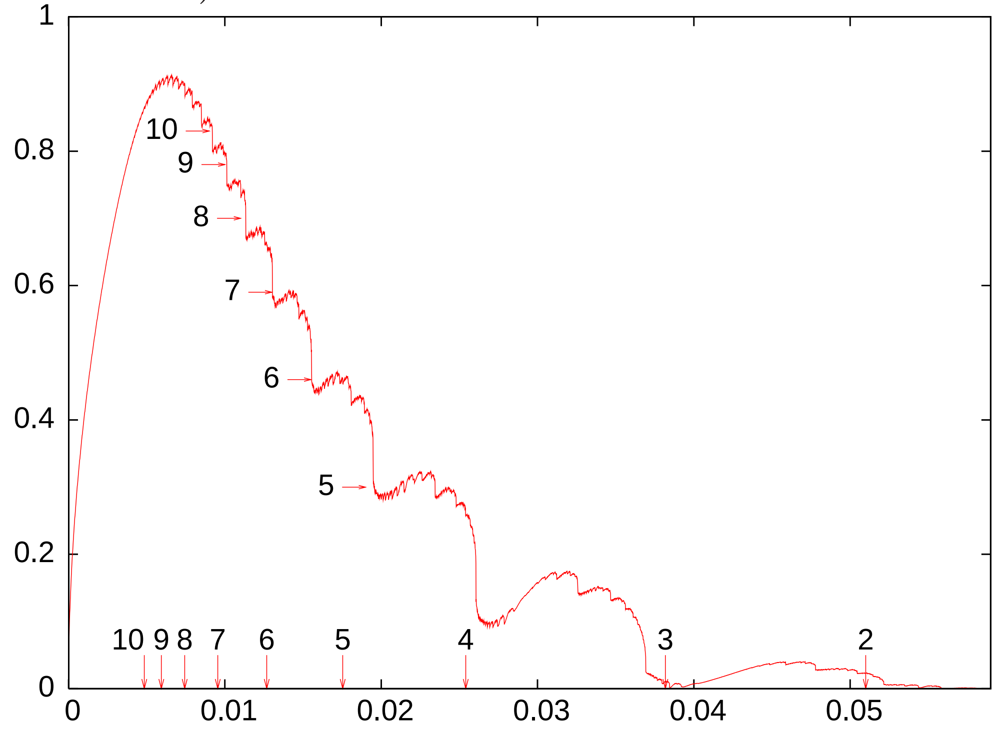

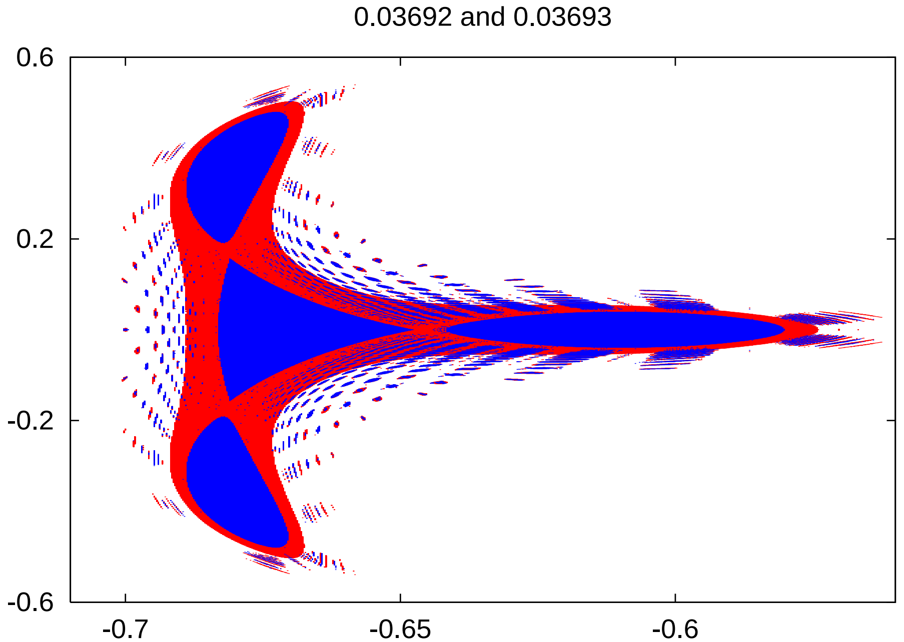
0.03692 and 0.03693
0.6
0.2
-0.2
-0.6
-0.7
-0.65
-0.6

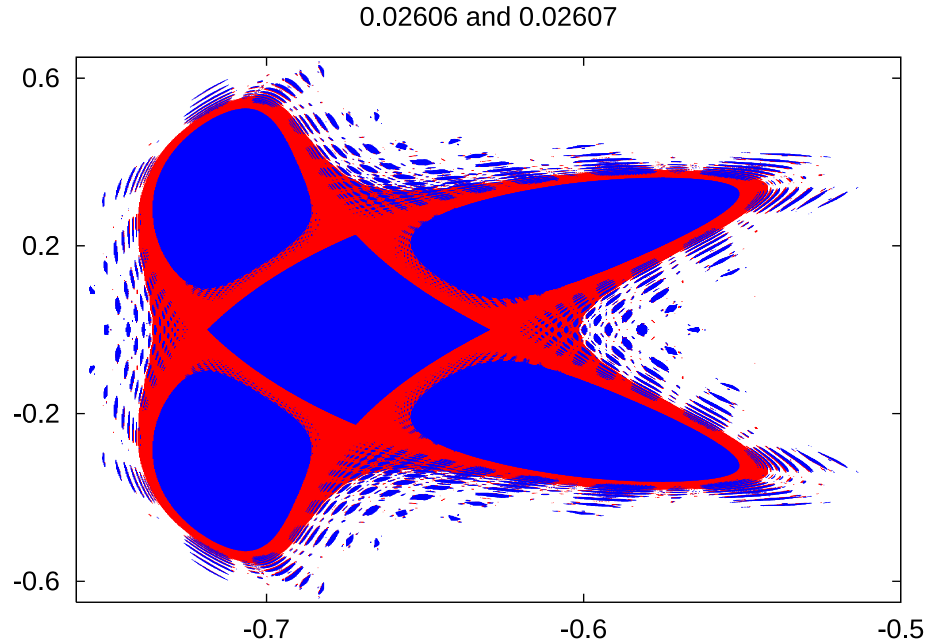
0.02606 and 0.02607
0.6
0.2
-0.2
-0.6
-0.7
-0.6
-0.5

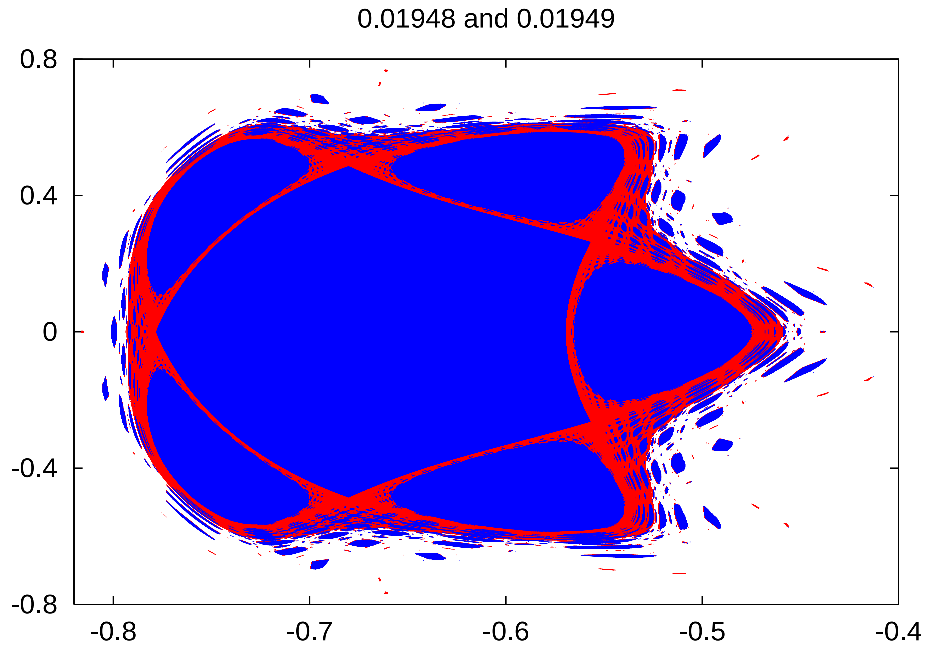
0.01948 and 0.01949
0.8
0.4
0
-0.4
-0.8
-0.8
-0.7
-0.6
-0.5
-0.4

Fluid mechanics: the Rayleigh-Bénard problem

Describes the **convection** forced by difference of temperature between bottom and top. We consider a **cube with conducting lateral walls**.

$$Pr^{-1}\left(\frac{\partial \boldsymbol{V}}{\partial t} + Ra^{1/2}(\boldsymbol{V}\cdot\boldsymbol{\nabla})\boldsymbol{V}\right) - \nabla^2 \boldsymbol{V} - Ra^{1/2}\theta\,\boldsymbol{e}_z + \boldsymbol{\nabla}\,p = 0\,,$$

$$\frac{\partial \theta}{\partial t} + Ra^{1/2}(\boldsymbol{V}\cdot\boldsymbol{\nabla})\theta - \nabla^2\theta - Ra^{1/2} w = 0\,, \qquad \boldsymbol{\nabla}\cdot\boldsymbol{V} = 0\,,$$

subject to boundary conditions $\boldsymbol{V} = \theta = 0$ at $|x| = |y| = |z| = 1/2\,.$

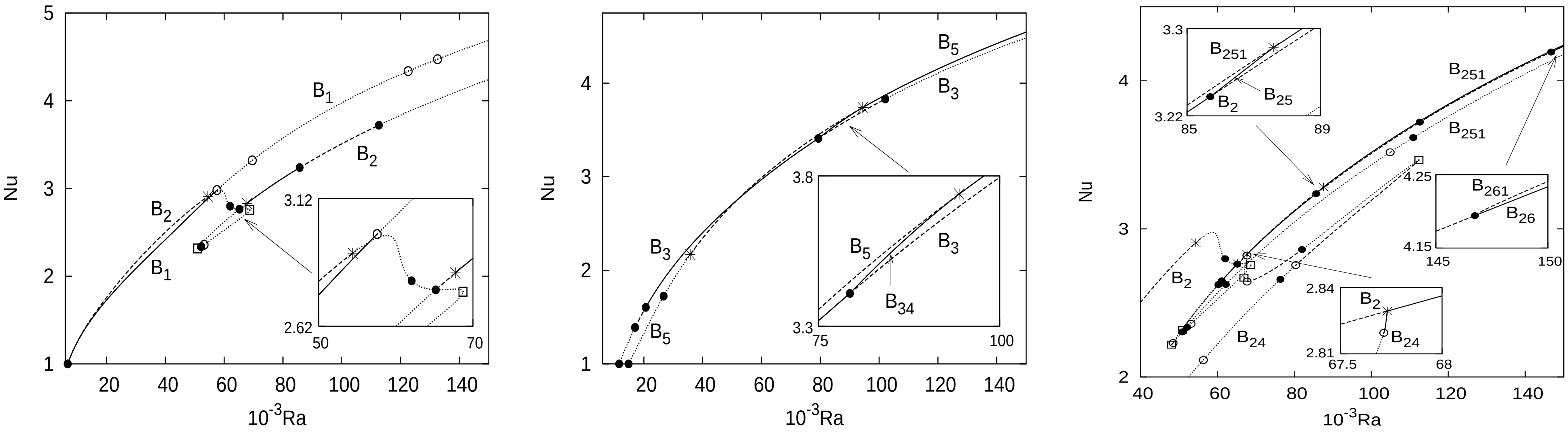

Parts of the bifurcation diagram of steady state solutions for $Pr = 130$. From Puigjaner, Herrero, S., Giralt, J. Fluid Mechanics, 2008.

On the left a sketch of the bifurcation diagram of steady state solutions up to 3 unstable directions is shown.

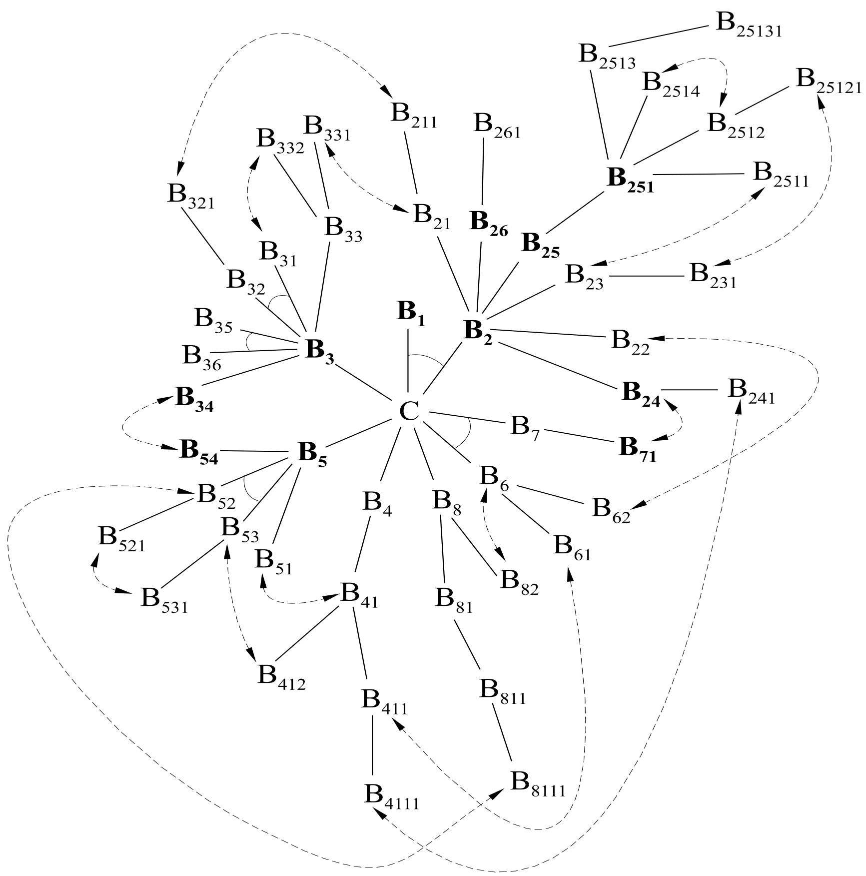

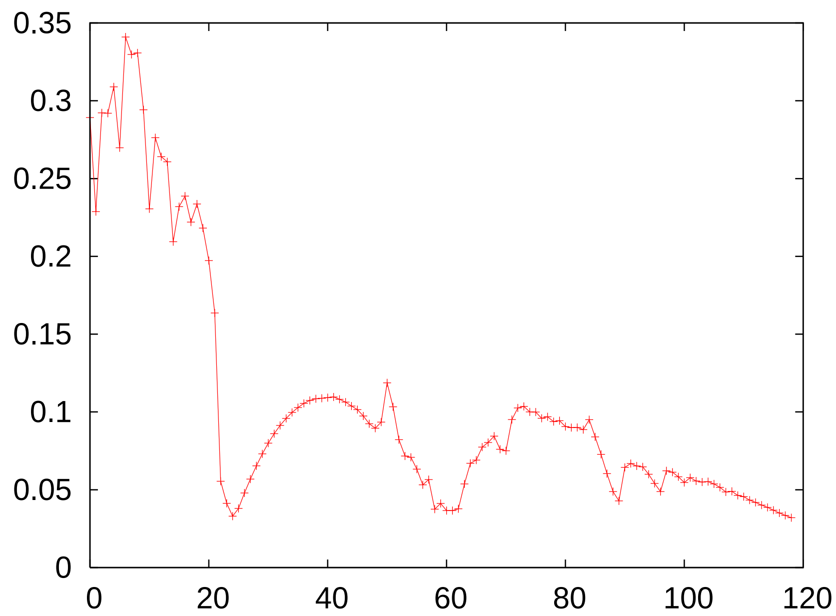

We are interested in dynamics of particles inside the cube. On the right: Example for B2 branch, where the horizontal coordinate displays a number of solution along the branch. The vertical coordinate shows the fraction of volume bounded by invariant tori.

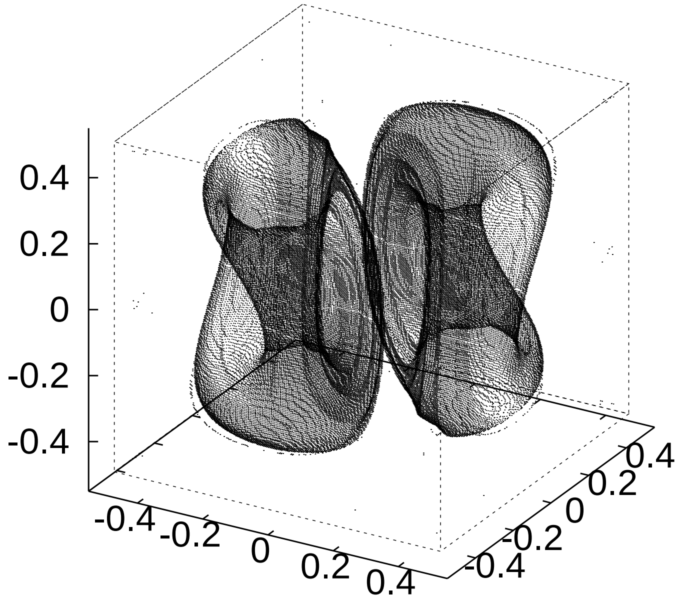

$Ra = 10^4$

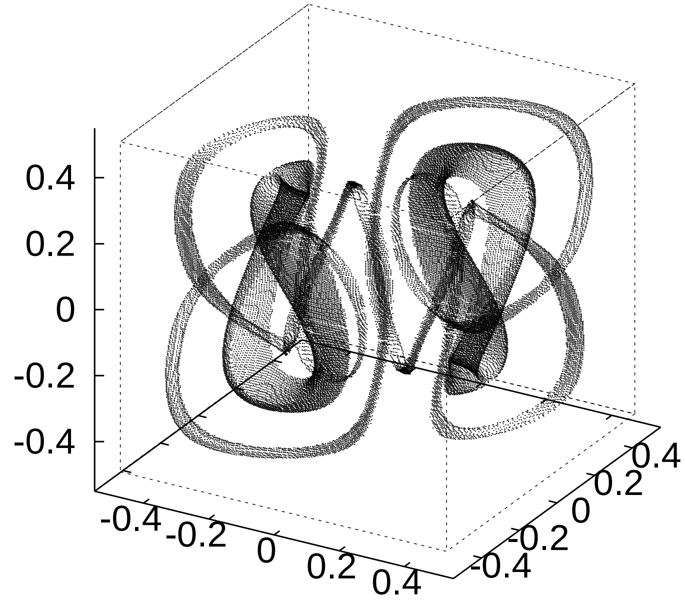

$Ra = 3.4 \times 10^4$

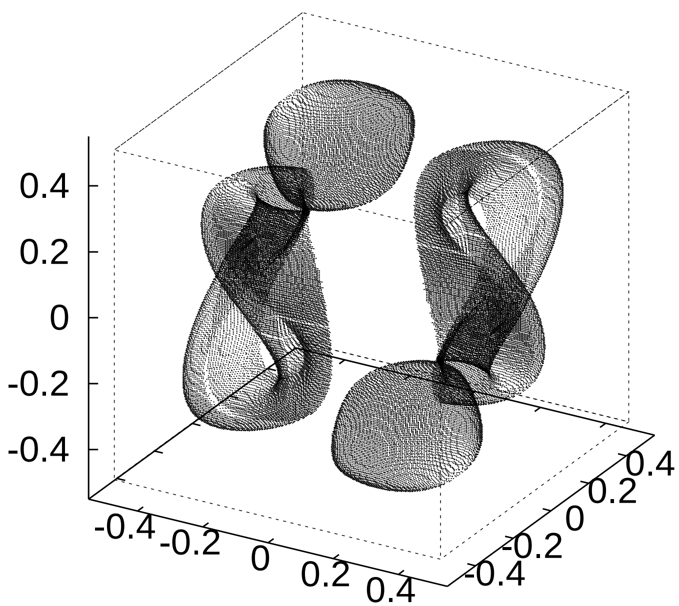

$Ra = 6 \times 10^4$

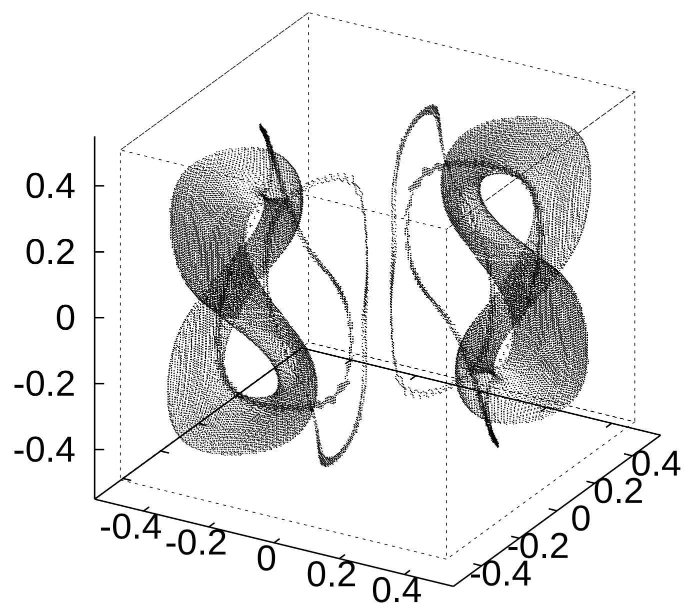

$Ra = 8.5 \times 10^4$

A paradigmatic example: the Hénon map

Any quadratic area preserving map can be reduced to

$$\begin{pmatrix} x \\ y \end{pmatrix} \rightarrow \begin{pmatrix} \bar{x} \\ \bar{y} \end{pmatrix} = \begin{pmatrix} c(1-x^2)+2x+y \\ -x \end{pmatrix} \qquad x, y, c \in \mathbb{R}.$$

With this normalisation **fixed points** at H$=(-1,1)$ and E$=(1,-1)$, **elliptic** if $c \in [0,2]$: $Tr(E) = 2-2c$. A **Normal Form** analysis proves **non linear stability** if $c \in (0,2) \setminus \{1.5\}$.

It appears typically in **generic non-hyperbolic area preserving maps**, e.g., in **Poincaré sections of Hamiltonian systems with two degrees of freedom** in **many parts of the phase space**.

Despite its trivial character still **many of its properties are not know in detail** mainly concerning **global aspects**.

It serves as **paradigm** for many phenomena. See S-Vieiro, Resonant zones, inner and outer splittings in generic and low order resonances of APM, preprint, and Global study of area preserving maps, in preparation.

Typical phase portrait and non-escaping points

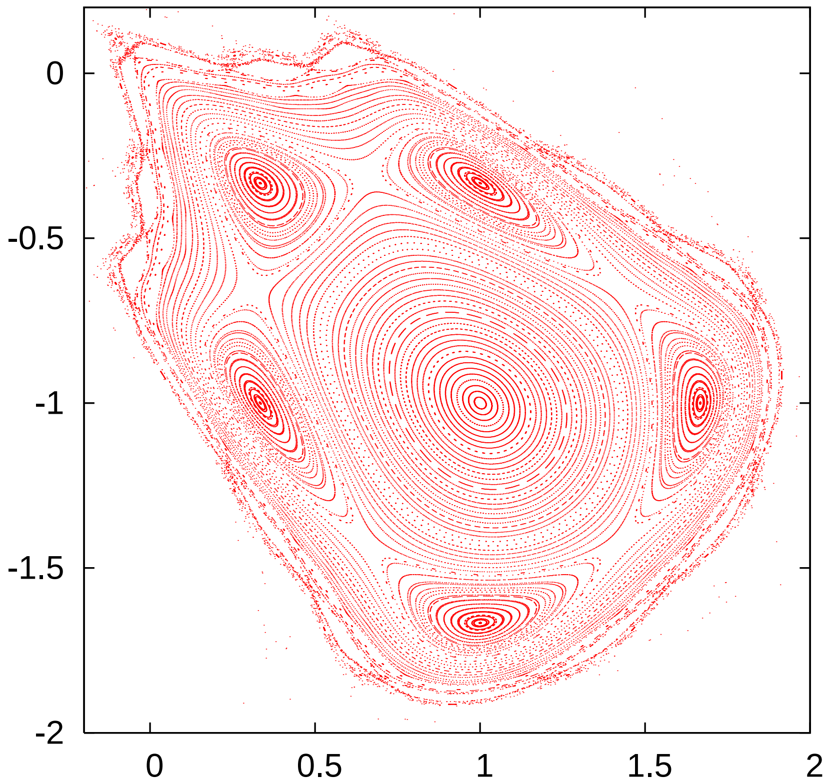

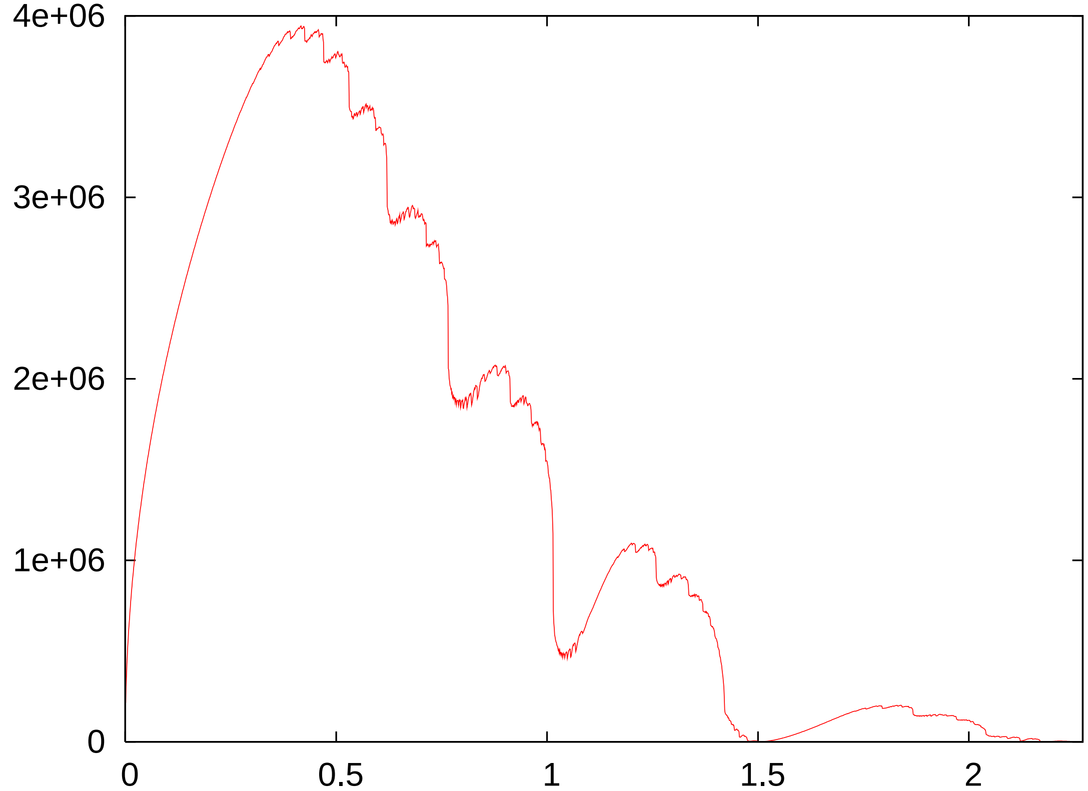

Left: **Phase portrait** for $c = 0.75$. Outside that domain, points **escape** to infinity, close to W_H^u. Right: number of **non-escaping points** on a grid $10^{-3} \times 10^{-3}$. Computations done by a combination of methods. Observe the **self-similar** character and the **jump discontinuities**. Also the non-escaping points **before and after** the **destruction of rotational i.c. confining islands** of periods 5,4,3.

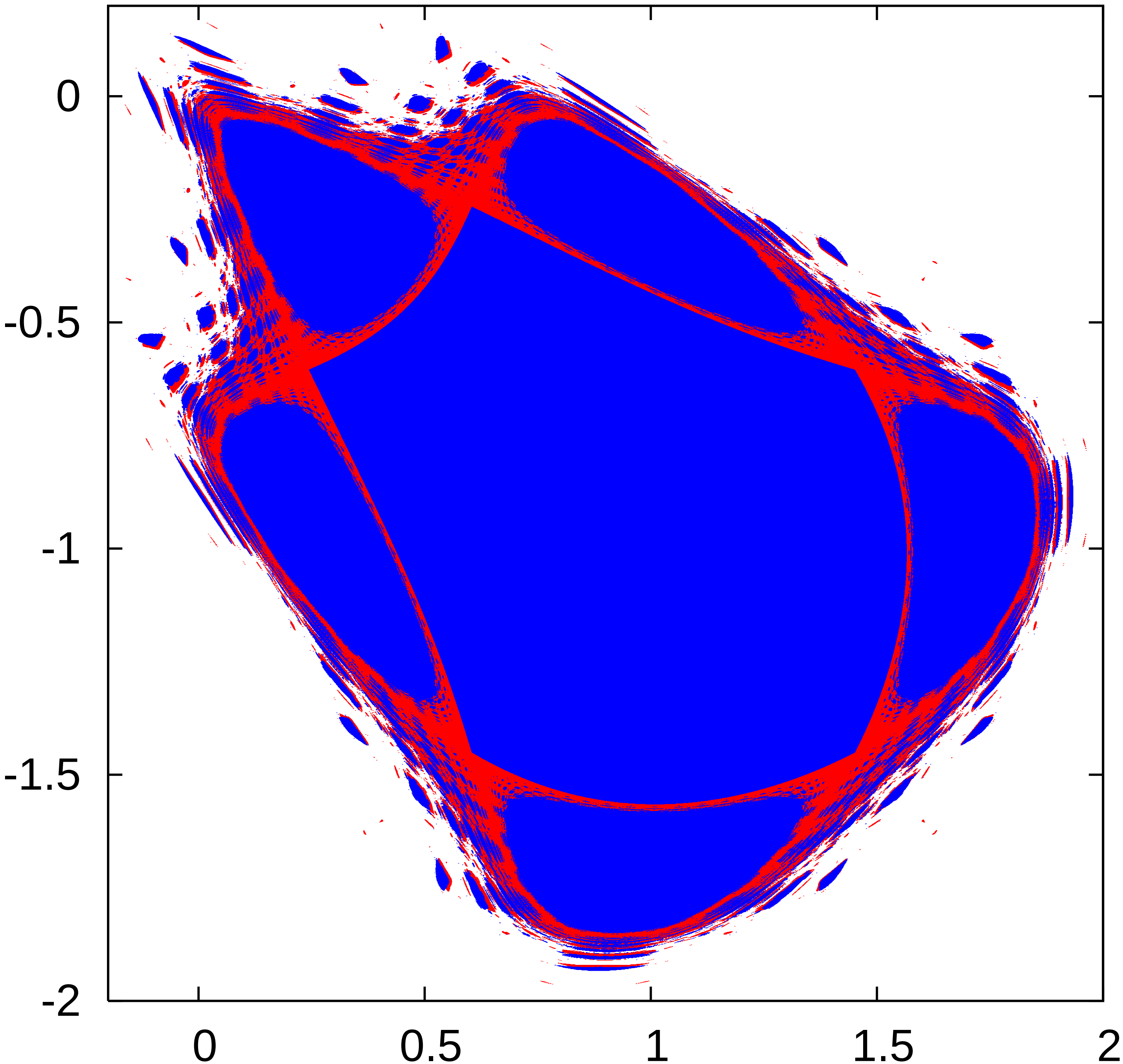
0
-0.5
-1
-1.5
-2
0
0.5
1
1.5
2

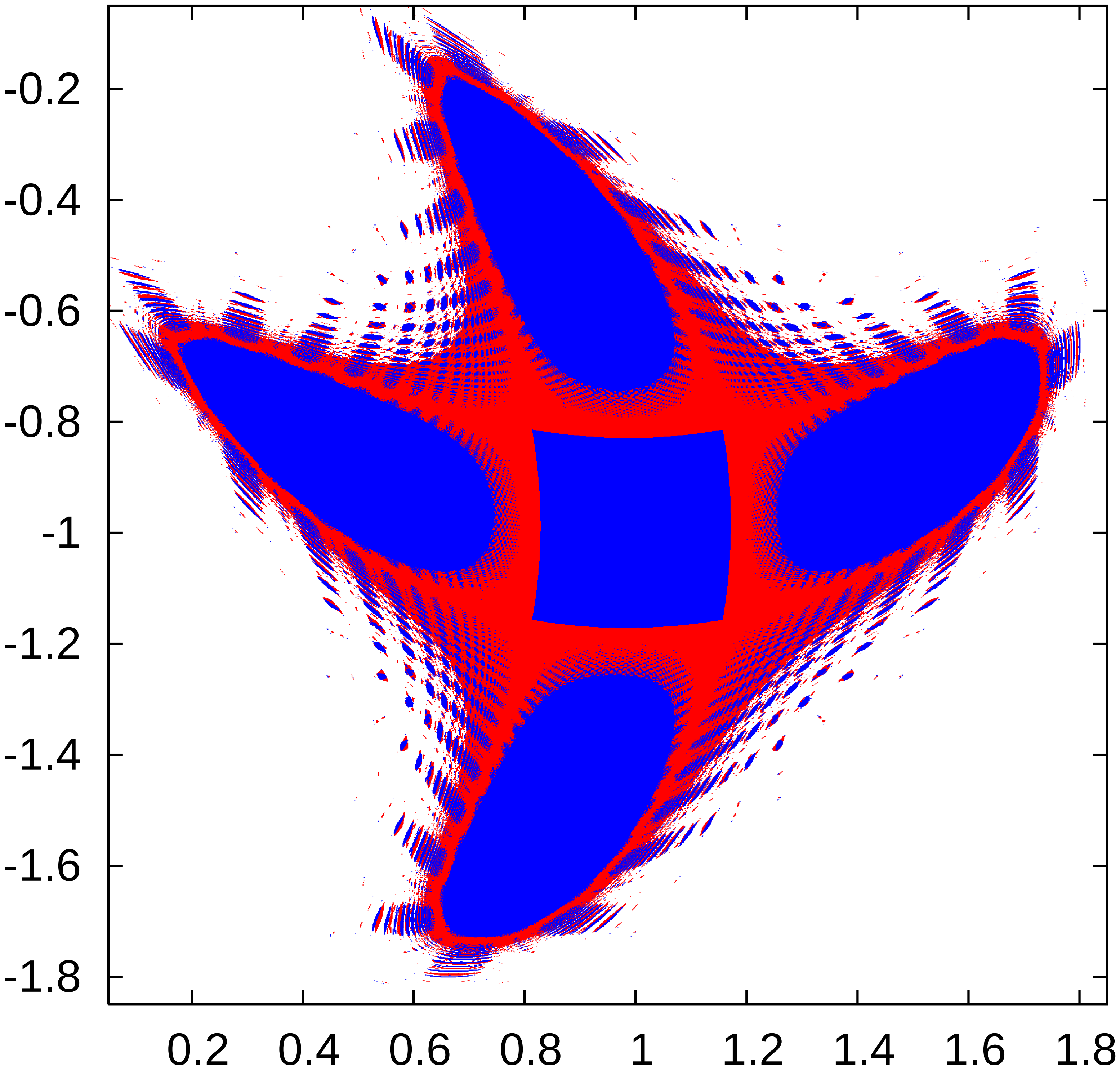

-0.2
-0.4
-0.6
-0.8
-1
-1.2
-1.4
-1.6
-1.8
0.2
0.4
0.6
0.8
1
1.2
1.4
1.6
1.8

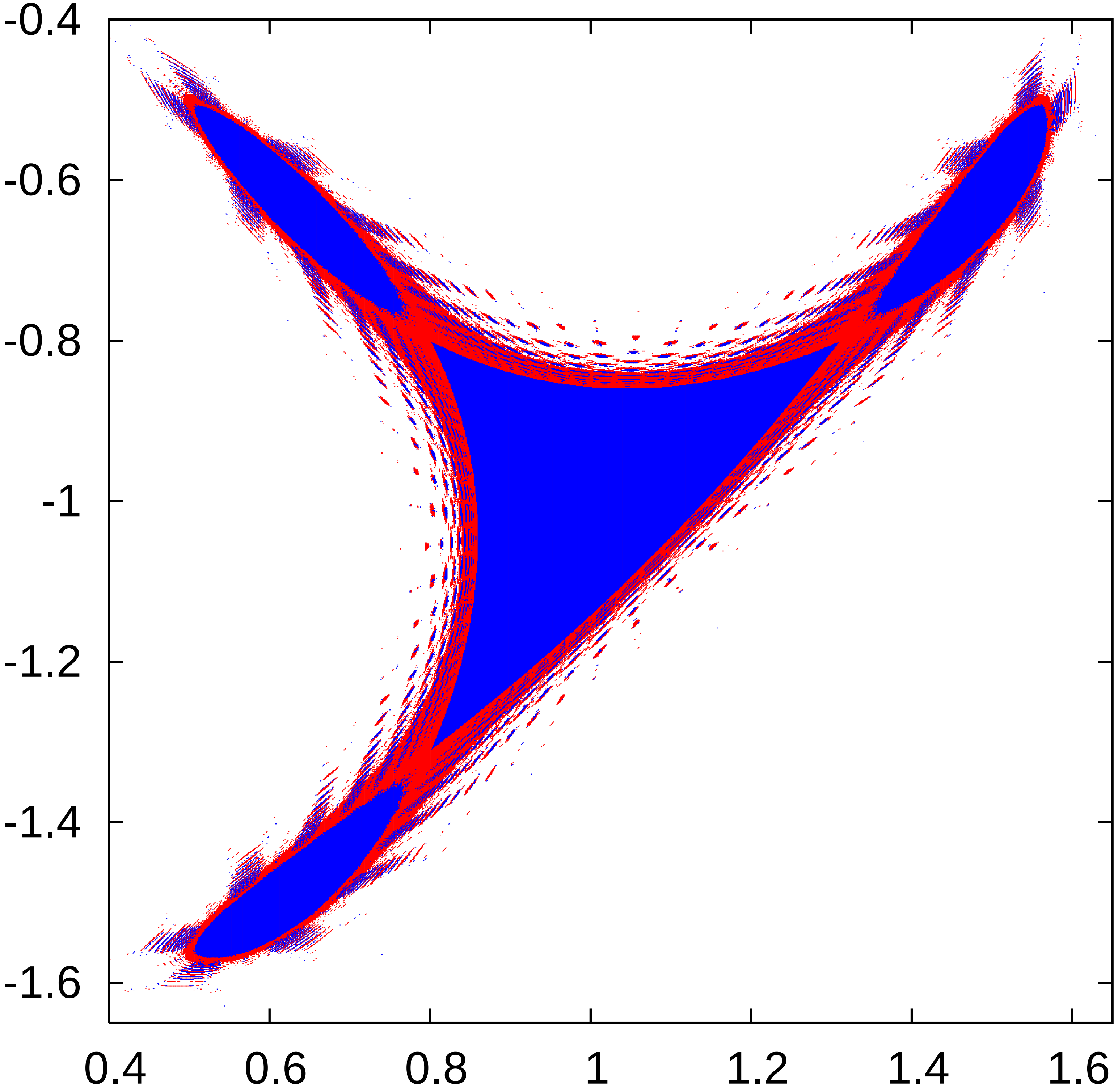
-0.4
-0.6
-0.8
-1
-1.2
-1.4
-1.6
0.4
0.6
0.8
1
1.2
1.4
1.6

Analytic tools

KAM theory: conditions for applicability

Twist map: $T : (r, \theta) \mapsto (r, \theta + \alpha(r)), \quad d\alpha/dr \neq 0$ on $a \leq r \leq b, \theta \in \mathbb{S}^1$. Then

Theorem (KAM). Consider an APM perturbed twist map $T_\varepsilon : (r, \theta) \mapsto (r + \varepsilon f_1(r, \theta, \varepsilon), \theta + \alpha(r) + \varepsilon f_2(r, \theta, \varepsilon)$. If

- $d\alpha/dr \neq 0$ for T, **frequency changes with amplitude**,
- The **rotation number** ρ of an invariant curve of T satisfies a **Diophantine Condition DC,** $|q\rho - p| > c|q|^{-\tau}$, for some $c > 0, \tau \geq 1$,
- The **perturbation** $||\varepsilon f||$ is **sufficiently small**,

then T_ε has a nearby i.c. with the given ρ.

The three conditions are not independent: **the larger** $|d\alpha/dr|$ **and the DC, the larger the admissible perturbation can be**.

"Best" ρ: Noble numbers.

Generalises to maps in a product of annuli.

The splitting of separatrices

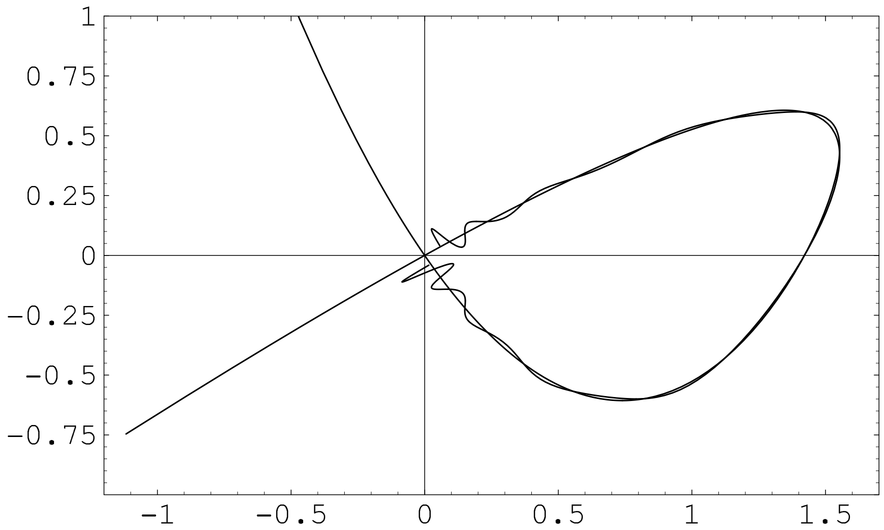

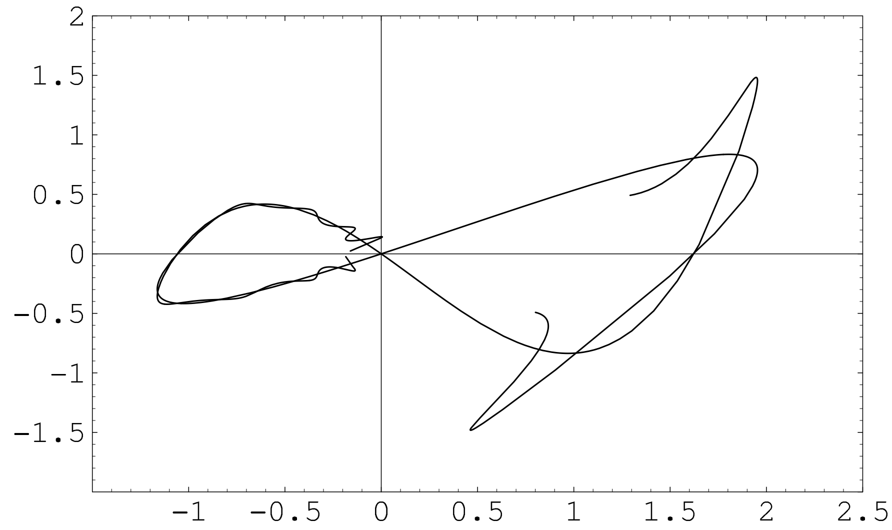

First upper bounds

Averaging theorem (Neishtadt). Given $z' = \varepsilon f(z,t,\varepsilon)$ with g analytic w.r.t. $z \in K$, compact in $\mathbb{C}^m$, 2π-periodic in t, bounded in ε, there exists a change $z = h(w,t,\varepsilon)$, such that $w' = \varepsilon g(w,\varepsilon) + r(w,t,\varepsilon)$ with $||r|| < \exp(-d/\varepsilon)$, $d > 0$.

Extends (S) to the case of f quasi-periodic in t with s frequencies satisfying a DC $(k,\omega) \geq c|k|^{-\tau}$, $\forall k \in \mathbb{Z}^s \setminus \{0\}$. Then $||r|| < \exp(-d/\varepsilon^{1/(\tau+1)})$.

Sharp upper bounds

Let

- $\mathcal{H}(q,p)$ a 1 dof (analytic) Hamiltonian with an **homoclinic orbit** $\gamma(t)$ to an hyperbolic point H,
- σ the smallest absolute value of the **imaginary part of the singularities** of γ,
- T_ε an analytic APM: $T_\varepsilon = \varphi_\varepsilon^{\mathcal{H}} + \mathcal{O}(\varepsilon^2)$,
- $h = \ln(\lambda(\varepsilon))$, being $\lambda(\varepsilon)$ the dominant eigenvalue of T_ε at the hyperbolic point H_ε.

Theorem (Fontich-S). $\forall \delta > 0$ exists $N(\delta)$ s.t. the size of the splitting $< N(\delta)\exp(-(2\pi\sigma-\delta)/h)$.

Generically the **asymptotic size of the splitting** is of the forms

$$Ah^r \exp(-2\pi\sigma/h)(1+o(1)), \quad Ah^r \exp(-2\pi\sigma/h)\left(\sum_i \cos(g_i/h+\xi_i)+o(1)\right)$$

as $\varepsilon \to 0$. (See Lazutkin, Gelfreich, Gelfreich-S).

Inner and outer splitting at a resonance

T twist map, $r_{m/n}$ such that $\alpha(r_{m/n}) = m/n$ (resonant circle). Sketch of a resonance for an APM. Generically separatrices **split** near p (**outer splitting**) and near q (**inner splitting**).

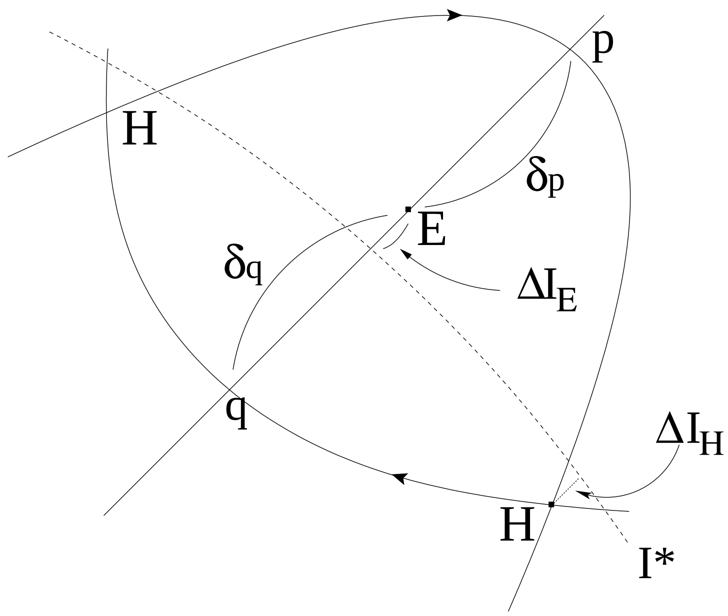

Resonant NF: $z \mapsto R_{2\pi\frac{m}{n}}(e^{2\pi i\gamma(|z|)}z + c\bar{z}^{n-1} + \hat{\mathcal{R}}_n(z,\bar{z}))$

$\gamma(|z|) = \delta + b_1|z|^2 + b_2|z|^4 + \ldots, \quad b_j$ Birkhoff coefficients.

Theorem (S-Vieiro). Assume $b_1, b_2 \neq 0$. Then, inner and outer splittings for the m/n resonance have, generically, **different σ parameters**. For δ small they depend mainly on b_1, b_2.

In a general T_ε, b_1, b_2 are replaced by $d\alpha/dr|_{r_{m/n}}$, $d^2\alpha/dr^2|_{r_{m/n}}$.

Hence these splittings are of **quite different order of magnitude** for δ or ε small.

Key models and return maps

Return maps are essential to understand global phenomena. Consider the behaviour near a **broken separatrix**, either single loop or figure 8. A model can be derived by considering **passage close to the saddle** and **gluing maps**.

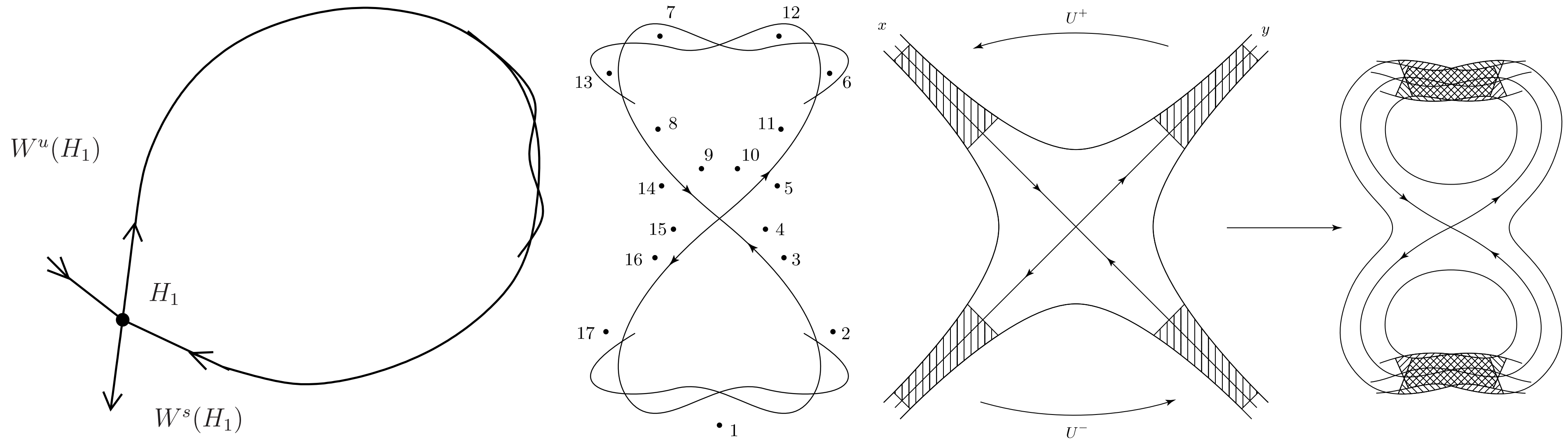

A **general separatrix map** and relevant universal properties has been studied in S-Treschev. As a simple (and typical) case we have the **Chirikov separatrix map**, which scaling actions by the size of the splitting and identifying lower and upper parts reads

$$SPM \begin{pmatrix} x \\ y \end{pmatrix} = \begin{pmatrix} \bar{x} \\ \bar{y} \end{pmatrix} = \begin{pmatrix} x + a + b\log(|\bar{y}|) \\ y + \sin(2\pi x) \end{pmatrix}.$$

For b large SPM looks quite chaotic near $y = 0$. It seems that **inside the lobes** the dynamics is **fully chaotic**, but it has been proved that the fraction of ε (in log scale) for which there are stable islands inside the lobe, tends to **a positive constant** if $\varepsilon \to 0$ (Broer-S-Tatjer, S-Treschev and S-Vieiro).

Theorem: The SPM has only **invariant rotational curves** (i.e., graphs of $y = g(x)$) if $\frac{b}{y_0} < \varepsilon_G$, where $\varepsilon_G \approx 0.9716/(2\pi)$, the so-called **Greene's critical value**.

Thanks to contributions of Chirikov, Greene, Mather, MacKay, Rana-de la Llave, Olvera-S, based on analysis of the standard map SM.

For some cases, like the transition for $c \in [1.014, 1.015]$ in the Hénon map there are **chains of islands**, the first and last ones very narrow and become larger in the central part. The SPM is not a good model for this.

Not only one but **two separatrices** play a relevant role in the creation of these islands. A similar thing occurs in the **Birkhoff zones**. The simplest model is the **biseparatrix map**, which for $0 < y < d$ is given by

$$BSPM \begin{pmatrix} x \\ y \end{pmatrix} = \begin{pmatrix} \bar{x} \\ \bar{y} \end{pmatrix} = \begin{pmatrix} x + a + b_1 \log(\bar{y}) - b_2 \log(d - \bar{y}) \\ y + \sin(2\pi x) \end{pmatrix}.$$

where $d, b_1, b_2 > 0$ and x mod 1. A suitable scheme is shown.

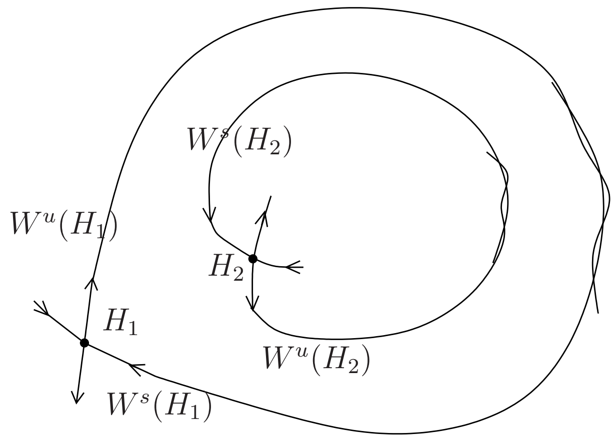

Theorem (S.-Vieiro): The condition **to exist rotational invariant curves** for the BSPM can be written as $\dfrac{b_1}{y_0} + \dfrac{b_2}{d - y_0} < \varepsilon_G$. In particular, there are no such i.c. if $(\sqrt{b_1} + \sqrt{b_2})^2/d > \varepsilon_G$.

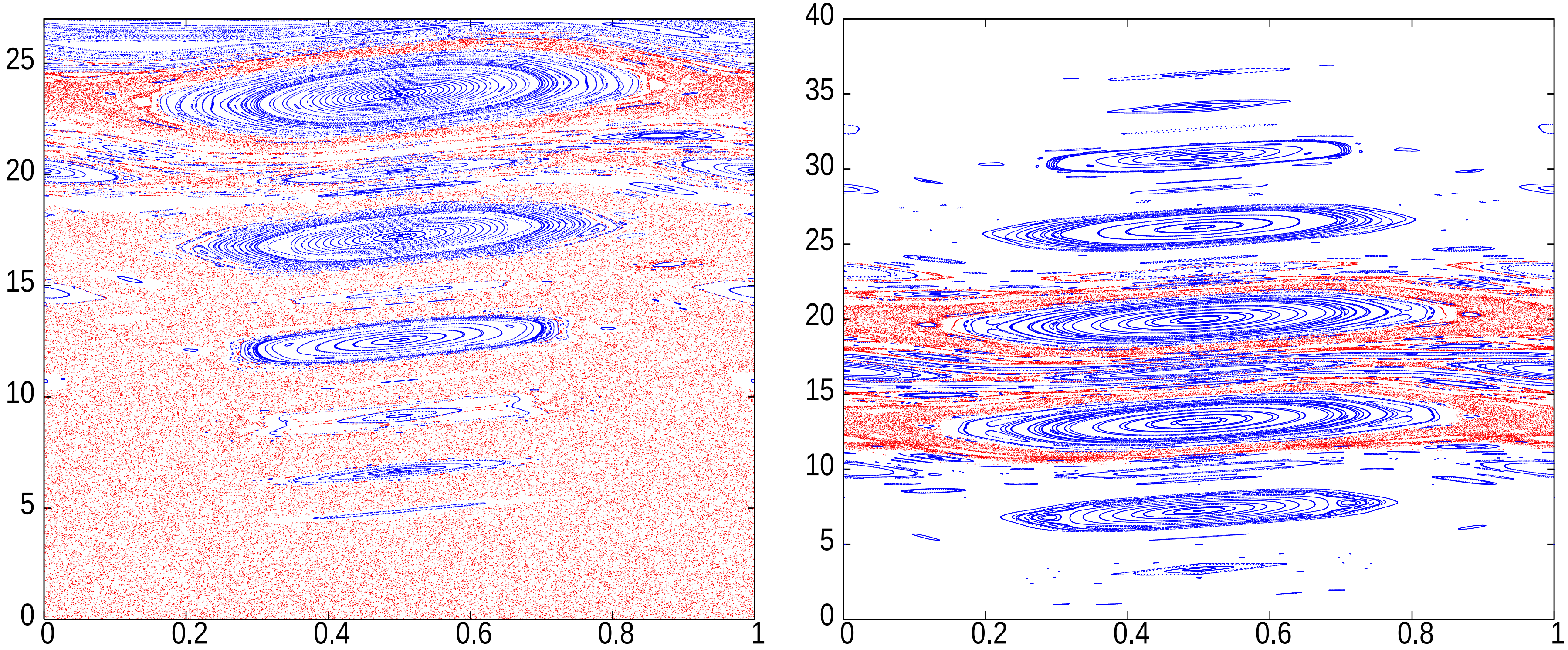

Left: an example of the SPM for $a = 0$, $b = \sqrt{10}$. Positive Lyapunov exponent in red. Zero Lyapunov exponent in blue. Right: an example of the $BSPM$ for $a = 0$, $b_1 = 1$, $b_2 = 3$, $d = 40$.

Computational tools

Long time integrations: Taylor methods

Consider an IVP f analytic in a nbd of $(t_0, x_0) \in \Omega \subset \mathbb{R} \times \mathbb{R}^n$

$$\dot{x} = f(t, x), \qquad x(t_0) = x_0.$$

We want to produce **in an easy way** the **Taylor expansion** $x(t_0 + h)$ to high order for suitable h and use it as a one-step method. Easy to implement, accurate and fast using **automatic differentiation methods** and **truncation errors τ largely below roundoff**

Theorem. For a very large class of analytic, non-stiff, ODE the Taylor method has the following properties:
- Asymptotically, for small enough τ, the **optimal step size** (concerning efficiency) is almost independent of the number of digits and equal to $\rho(t)/\exp(2)$, where $\rho(t)$ is the local radius of convergence.
- The **optimal order** is approximately linear in the number of digits.
- For a given equation and fixed t_0, t_f, the **global computational cost**, is $O(D^4)$, where D is the number of digits.

Example of energy change in Sun-Jupiter-asteroid model. Asteroid in a large domain around L_4. Of a total of 175 test particles 43% subsisted for 10^9 Jupiter revolutions ($\approx$ **twice the age of Solar System**). The two worst cases are displayed. Initial energy is of the order of units.
System **S-J-S-U-N** for **4.5 Gyr**: $\Delta H/H < 10^{-11}$. CPU time:**3 days**.

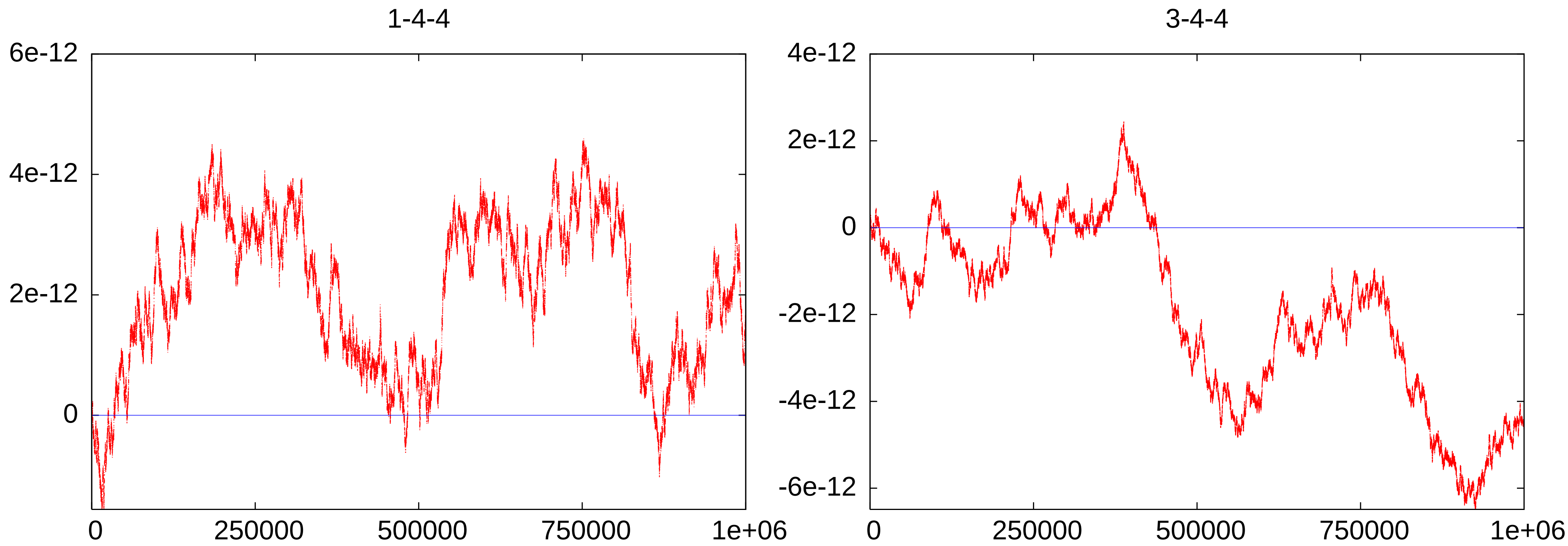

Assuming **iid random roundoff errors** the effect is $O(t^{1/2})$ in first integrals and, for integrable systems, is $O(t^{3/2})$ in angles.

Dynamics indicators: Lyapunov exponents

Given $x_0, v_0, |v_0| = 1, S_0 = 0$ compute

$$x_{k+1} = T(x_k), \qquad w_{k+1} = DT(x_k)(v_k),$$

$$v_{k+1} = w_{k+1}/|w_{k+1}|, \qquad S_{k+1} = S_k + \log |w_{k+1}|.$$

Then the limit slope of S_k as function of k gives Λ_{max}

Comments:

- Use **smoothing, fitting, extrapolation, self consistency** to compute Λ_{max}.

- Stop at **right place** x_N close to x_0 to improve estimates.

- Use alternative estimators (e.g. **MEGNO**) for near-integrable.

- Possible determination of **all exponents**

See Broer-S, Cincotta-S, Cincotta-Giordano-S, Ledrappier-Shub-S-Wilkinson.

Dynamics indicators: frequency analysis

Given samples $\{f(jT/N)\}_{j=0}^{N-1}$ of $f(t)$ on $[0,T]$, determine a trigonometric polynomial,

$$\mathbf{Q_f(t) = A_0^c + \sum_{l=1}^{N_f} \big(A_l^c \cos(2\pi\nu_l t/T) + A_l^s \sin(2\pi\nu_l t/T) \big)}$$

whose **frequencies**, $\{\nu_l\}_{l=1}^{N_f}$, and **amplitudes**, $\{A_l^c\}_{l=0}^{N_f}$, $\{A_l^s\}_{l=1}^{N_f}$, are a good approximation of the corresponding ones of $f(t)$. N_f, to be determined by the procedure (in terms of some input parameters). Like N_f as small as possible, keeping high accuracy in the computed $\nu_l, A_l^{c,s}$.

Key ideas of the procedure: a decreasing set of thresholds and a convergent Newton method to compute $\nu_l, A_l^{c,s}$.

Theorem (Gómez-Mondelo-S). If f is analytic, quasi-periodic with Diophantine frequencies, there exist **explicit formulas for the errors** in $\nu_l, A_l^{c,s}$, depending on
Cauchy estimates for f, Diophantine constants, T and N.

Computing qp invariant curves

Working with a Fourier representation

Assume $x(t) = \sum_{k \in K} c_k \exp(k\mathrm{i}\, t)$, $t \in \mathbb{S}^1$ is a representation of the curve for some set of indices K. Then

a) Look for **invariance**: Take a grid $\{x(2\pi j/N)\}$, compute images $\{T(x(2\pi j/N))\}$, analyse them and impose to have same c_k, or

b) Look for **conjugation**: Search a transformation $\mathbb{C}$ which conjugates T to a rotation.

In both cases use a normalisation, because of the arbitrariness of the origin.

Working in phase space

Select a line $\mathcal{L}$ transversal to the curve and an initial p on it. Compute iterates and take some which return close to p. Interpolate them to find a point q in $\mathcal{L}$. Impose $q = p$ and solve w.r.t. p.

Curve fitting

Question: Given a point p, is it on an invariant curve for T?

1) Compute **iterates** of p and keep the ones close to p.
2) **Fit a curve** to the iterates in some local coordinates. Use orthogonal polynomials with respect to the set of abscissae.
3) Find **residuals**: size and distribution as a function of number of iterate.
4) Use some **test of acceptance** based on standard deviation.

An example: the outer cometary problem

Consider the **planar circular RTBP** with primaries **Sun-Jupiter**, located at $(\mu, 0)$, $(\mu-1, 0)$ in synodic (rotating) coordinates. $\mu \approx 1/1047.3486$.

Question: Given a value of the **Jacobi constant** C and considering motions **external to Jupiter's orbit** where is the **"last" invariant curve** which **prevents from escape**?

How it is evolving with C?

What about dependence in μ?

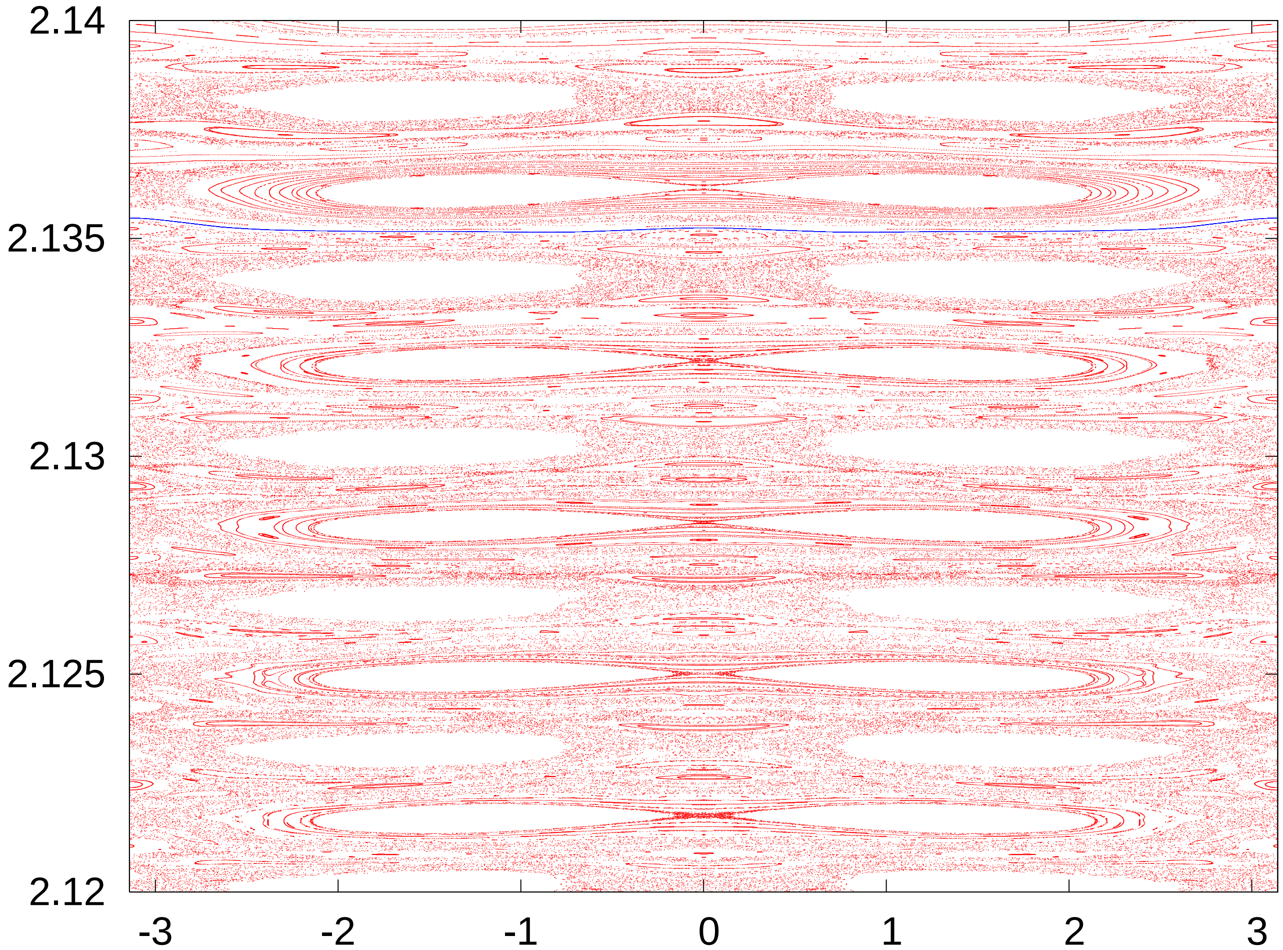

Poincaré section using **pericentre passages**: radius as a function of angle. Several initial conditions and 1000 iterates for each one. In blue: **approximate last invariant curve**. Jacobi $C = 4$.

$C = 1/a_{osc} + 2a_{osc}^{1/2}(1 - e_{osc}^2)^{1/2}$, $\quad a_{osc} \approx 9.55858, \quad e_{osc} \approx 0.77661,$
$q_{osc} \approx 2.13524, \quad T_{osc} \approx 185.682$

Details on curve, magnification, fit errors and evolution with iterates.

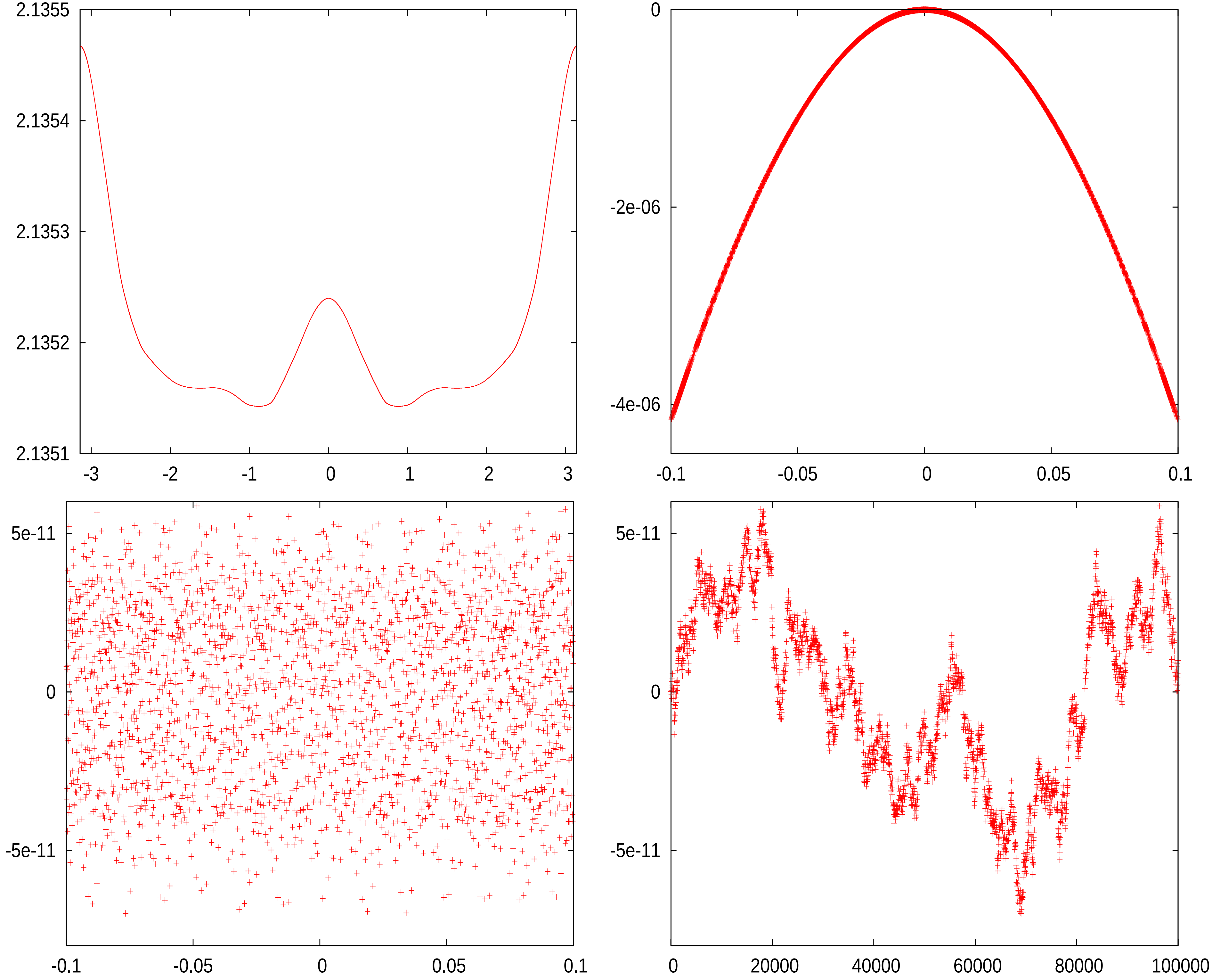

2.1355
2.1354
2.1353
2.1352
2.1351
-3
-2
-1
0
1
2
3
0
-2e-06
-4e-06
-0.1
-0.05
0
0.05
0.1
5e-11
0
-5e-11
-0.1
-0.05
0
0.05
0.1
5e-11
0
-5e-11
0
20000
40000
60000
80000
100000

Some details on the Hénon map

A general overview

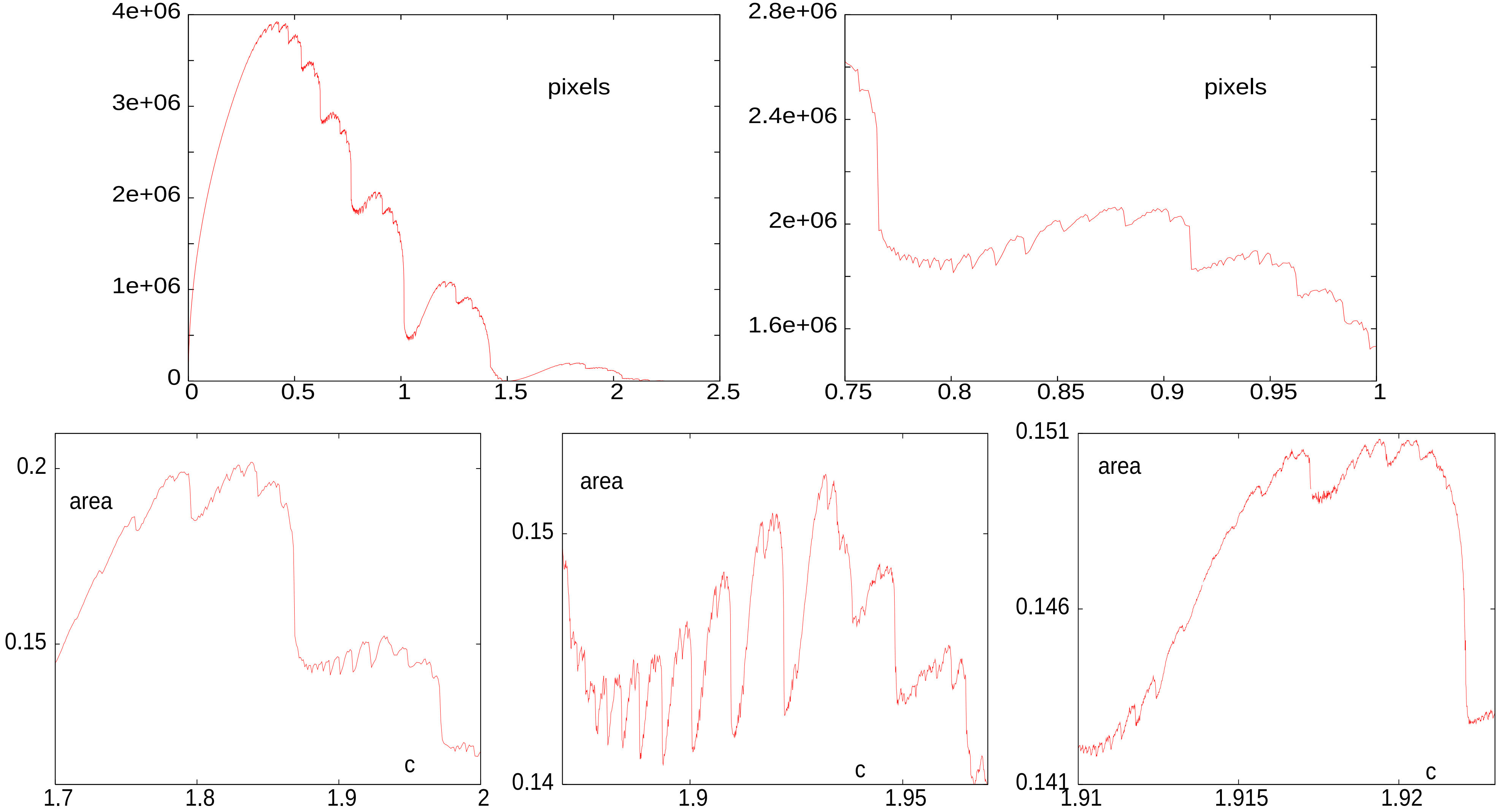

Statistics of results and some details.

Near-integrable case

Consider first c **small**. The map can be approximated by a **flow**.
Let $d = \sqrt{c/\sqrt{2}}$. The changes

$$\begin{pmatrix} x \\ y \end{pmatrix} = \frac{1}{\sqrt{2}} \begin{pmatrix} q+p \\ q-p \end{pmatrix}, \quad \begin{pmatrix} p \\ q \end{pmatrix} = \begin{pmatrix} u \\ dv \end{pmatrix}$$

allow us to write the **close to the identity map**

$$\begin{pmatrix} u \\ v \end{pmatrix} \longrightarrow \begin{pmatrix} u + 2dv + O(d^2) \\ v + d(1 - \frac{1}{2}u^2) + O(d^2). \end{pmatrix}$$

This map is $\mathcal{O}(d^2)$-close to the time d flow of Hamiltonian $K(u,v) = v^2 - u + \frac{1}{6}u^3$. The level $K = \frac{2}{3}\sqrt{2}$ containing the hyperbolic point $u = -\sqrt{2}, v = 0$ corresponds to a **separatrix**, enclosing the elliptic point $u = \sqrt{2}, v = 0$. The **splitting** for the manifolds of the map is **exponentially small in d.**

Also **invariant curves** of the map exist at an **exponentially small** distance of the manifolds.

A low-order resonance

As an example consider the parameter $c = 1.015$, just after the **destruction of the i.c. confining islands of period 4**. One can see a **domain without subsisting points** close to the **invariant manifolds** of the period 4 orbit, see upper plot in next page. It looks as if the manifolds coincide, at this resolution.

A computation of the splitting angle **in the outer and inner homoclinic connections** gives the values $s_o \approx -0.951063 \times 10^{-2}$, $s_i \approx 0.294215 \times 10^{-58}$.
From this one can derive a **composed separatrix map** and predict the distance from the manifolds at which **stable islands and invariant curves** appear in the domain bounded by the initial pieces of the manifolds. These values agree with the results obtained by **direct simulation**, but one should be careful about **how this depends on the place where we look**. See lower plots.
For the **outer islands** and the **existence or not of i.c.** one requires the use of the $BSPM$. Locally, in what concerns nearby islands, one can approximate again by the SPM.

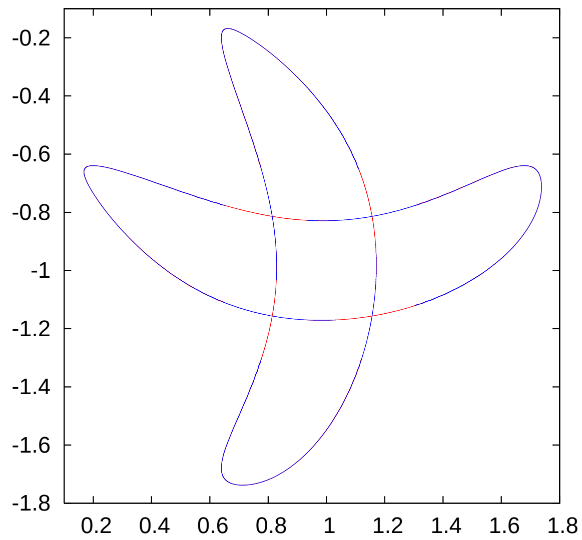

-0.2
-0.4
-0.6
-0.8
-1
-1.2
-1.4
-1.6
-1.8
0.2
0.4
0.6
0.8
1
1.2
1.4
1.6
1.8

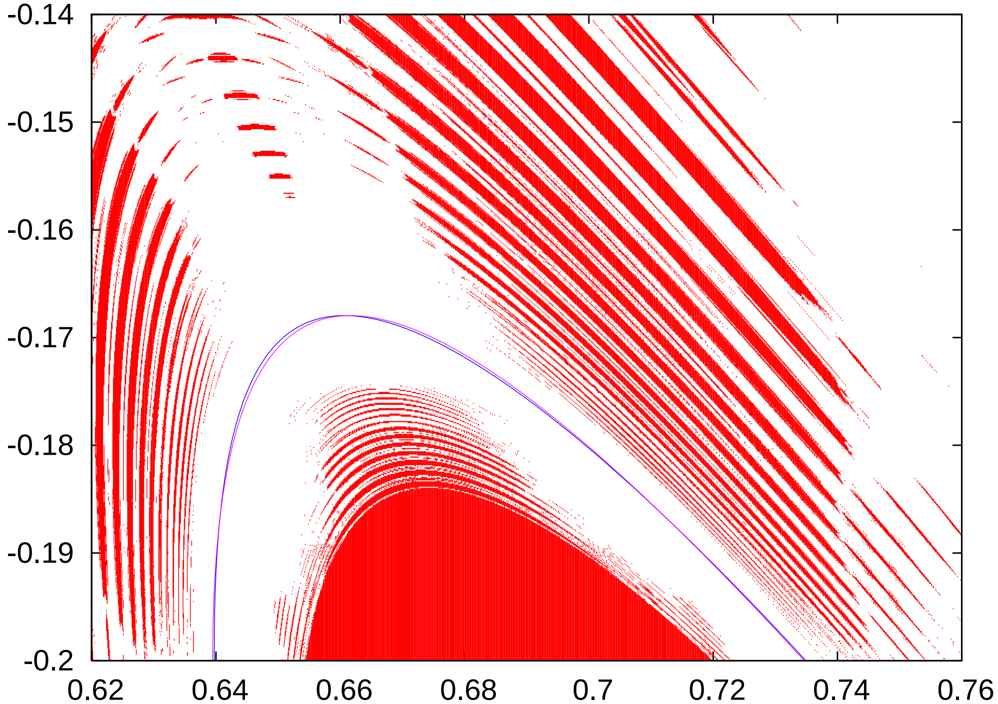

-0.14
-0.15
-0.16
-0.17
-0.18
-0.19
-0.2
0.62
0.64
0.66
0.68
0.7
0.72
0.74
0.76

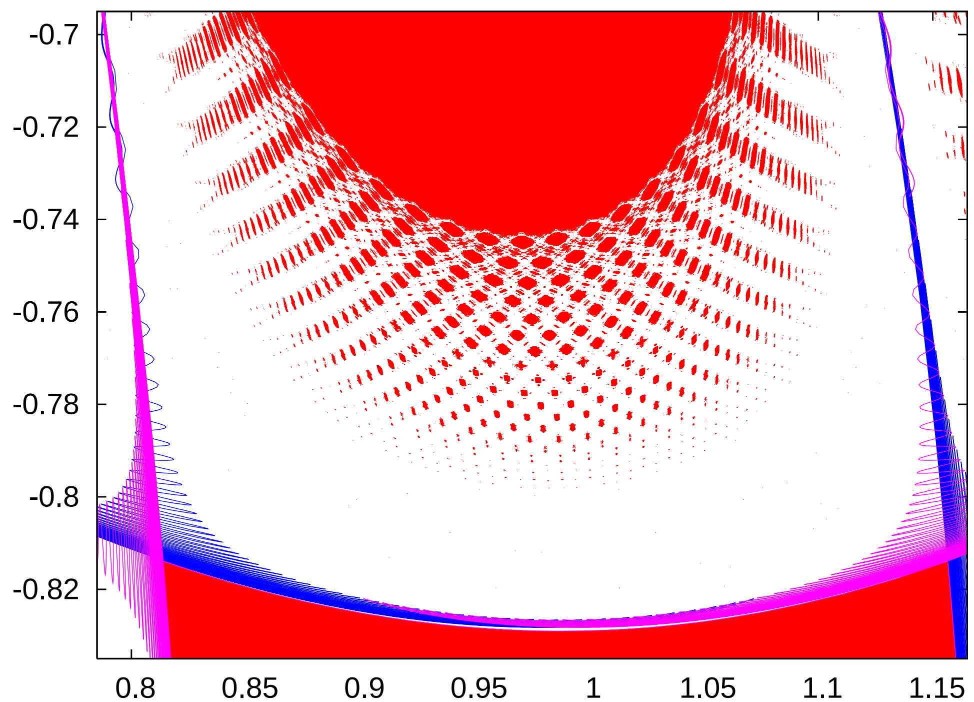

-0.7
-0.72
-0.74
-0.76
-0.78
-0.8
-0.82
0.8
0.85
0.9
0.95
1
1.05
1.1
1.15

Open problems and conclusions

- **Tools for higher dimensions**
- **The role of Cantor sets**
- **Escape and diffusion rates**
- **Conclusions**